27th EPS Conference on Contr. Fusion and Plasma Phys. Budapest, 12-16 June 2000 ECA Vol. **24B** *(2000) 308 -311*

Simulation of the RFX plasmas by the self-consistent code RITM.

G. Telesca[1], M.Z. Tokar[2]
[1]Consorzio RFX, Corso Stati Uniti,4 — 35127 Padova, Italy

[2]Institut fuer Plasmaptysik, Forschungszcntrum Juelich GmbH, EURATOM Association, D-52425 Juelich, Germany

1. Introduction.

In this paper we present first results of self-consistent transport modeling of plasmas in the reversed field pinch configuration. Standard discharges in the device RFX (R= 200 cm, a= 46 cm, plasma current I_p up to 1.2 MA, so far) have been simulated with and without neon seeding. Although many implications of the performed modeling have not yet been analysed in detail, the global behaviour of the main plasma and of the impurities as well as their scalings are satisfactory reproduced by the simulations. Some emphases has been put in describing the differences between neon seeded and non seeded discharges with the purpose of clarifying the interplay between changes in the impurity density and radiation and changes in transport. All the results, with the exception of the data of fig. 4, refer to plasma current I_p = 850 kA.

2. The RITM code

For modeling of the transport in RFX plasmas the code RITM (Radiation from Impurities in Transport Model) developed initially for description of tokamak discharges strongly influenced by impurities (see Ref.1,2) has been adapted to the configuration of RFP. The code RITM allows to model simultaneously the time evolution of the radial profiles for the densities of neutral and charged particles of the background hydrogen plasma and impurities, for the temperatures of electrons and ions, T*e,i*, and for the toroidal and poloidal components of the current density **J** and magnetic field **B**. The used model for hydrogen neutrals includes four species, namely, molecules, Franck-Condon, reflected and produced by charge-exchange atoms, and provides a sophisticated description of particle recycling at the last closed surface (LCMS). The continuity equation for electrons takes into account the transport channels through radial diffusion and convection and sources from the ionization of recycling neutrals and impurities. The latter are described in a consistent non-corona approximation by taking into account both transport and elementary processes like ionization, recombination, charge-exchange with hydrogen neutrals. This provides the density of radiation losses which is included into the equations for the heat balance of electrons together with the losses on the ionization of recycling neutrals, energy exchange with ions in coulomb collisions and ohmic heating with the power density Ω. To compute the latter the radial component of the plasma equilibrium equation, $\nabla P = 1/c\ [\mathbf{J} \times \mathbf{B}]$, and Maxwell equations in the Ùμ and *P*Ó[3] approximation are combined in an equation for the poloidal component of the magnetic field. Then according to Ref.3 $\Omega(r) = (I/\Phi)\ \eta(r)\ \mathbf{J}(r) \bullet \mathbf{B}$, where Φ is the total toroidal magnetic flux and η the Spitzer resistivity with the effective charge computed self-consistently with the densities of impurities. The boundary conditions at the LCMS are given by the e-folding lengths of densities and temperatures, taken from the measurements in the scrape-off layer.

The transport coefficients used in computations take into account that the main contribution to the energy and particles losses from RFX plasmas stems from the transport along stochastic magnetic field lines. According to theoretical models [5,6] the electron and ion heat diffusivities $\chi_{e,i}$ are given by different laws for collision free, $\lambda_c \geq \lambda_K$, and collisional, $\lambda_c \leq \lambda_K$, plasmas where λ_c and λ_K are the mean free path and Kolmogorov lengths, respectively. A collision

free situation is typical for the central plasma but at the plasma edge collisions dominate the transport. The latter explains the experimentally observed drastic decrease of $\chi_{e,i}$ when approaching the last closed magnetic surface. Both limit cases are unified in the formula $\chi_{e,i} = \chi_{\|,e,i}(B_r/B)^2 \times \min(1, \lambda_c/\lambda_K)$. The normalized magnetic fluctuation level, which is on the order of 1 —2 %, depends self-consistently on the plasma parameters, namely $\beta B \sim S^{-\alpha}$ where S is the Lunquist number (ratio of the resistive to Alfen times) and $\alpha = 0.35$. The diffusive component of particle transport, which is due to thermal motion along the stochastic field lines, is characterized by the coefficient $D_{eff}=c_s D_m$, where $c_s=[(T_e+T_i)/m_i]^{1/2}$. The convective particle flux, which is caused mainly by the temperature gradient, $\Gamma_{conv}=-n\times D_{eff}/(2T)\times dT/dr$, is outward directed for a normally peaked T_e profile. The transport of impurities in a stochastic magnetic field is more complex [7] and in this first study we have used a simple model with the impurity diffusivity equal to that of the main particles and the convective velocity $v_{imp}=-(r/a)\times 9$m/s. These impurity transport coefficients allow the experimental data to be reproduced satisfactorily.

3. Results (Radiation and particle transport)

In the following, RITM simulations of standard and neon seeded RFX discharges at plasma current Ip = 850 kA will be presented and discussed with respect to the underlying physics and to experimental observations. In fig.1 the profiles of the electron density, of Zeff and of the power radiated are shown for neon seeded and non-seeded discharges at central line average density n_{eo}=3 and 8 x 10^{13} cm $^{-3}$. The calculated profile of the radiated power density is quite comparable to the experimental one from bolometry at low and at high density both with and without Ne (note the different scales at low and at high density). Also the level of Zeff compares well with brems-strahlung measurements. As a result, the neon radiation efficiency, which is defined as $[P_{rad}/(Z_{eff}-1)]/n_e^2$ and which is found to be 2.3×10^{-39} MW m^6, is only about 20 % higher than that experimentally determined. (This difference might arise from the presence in the RFX plasmas of impurities other than C, O, Ne). Since the level of the radiation efficiency depends both on particle transport and on the electron temperature profile (heat transport), the agreement between experiment and simulations at two very different level of electron density gives a strong argument in favor of the transport model chosen. In fact the computed and measured total input power (ohmic) are very similar to each other. The electron temperature profile is parabolic with central and edge values of about 260 eV and 80 eV, respectively, for

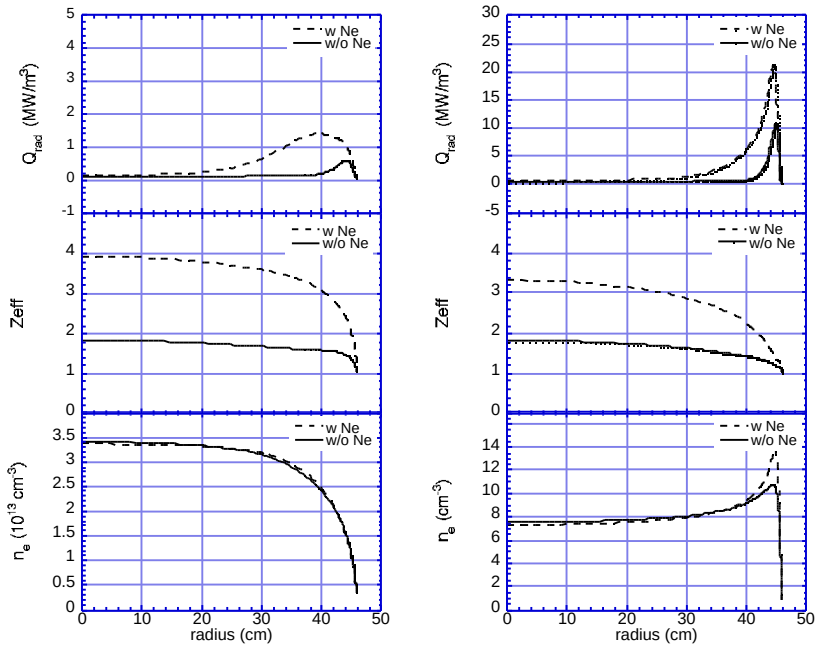

Fig1 Radiated power density,.Zeff and electron density without and with Ne at n_{eo}=3 (left) and $8x10^{13}cm^{-3}$ (right)

the low density case, and increases slightly with Ne seeding. At high density Te(0) is about 200 eV and Te(a) about 20 eV. As for the low density case it increases by about 10% in the center with Ne seeding, but decreases significantly at the plasma edge because the increase in the edge radiated power exceeds by far the increase in the total power input.

At n_{e0} = 3 x 10^{13}cm^{-3}the density profiles with and without Ne are practically identical and decrease monotonically toward the plasma edge. At n_{e0} = 8 x 10^{13}cm^{-3} they are hollow and in the Ne seeded case n_e is more peaked at the edge than in the standard situation. If the difference between hollow (high density) and bell-shaped (low density) profiles can mostly be understood in terms of differences in radial extension of the electronic source [8], a change in transport must be invoked to account for the differences at high density with and without Ne. In fact, although the injection of Ne in highly density discharges is associated with enhanced total particle fluxes _, it causes also an increase of the temperature gradient at the plasma edge (see fig.2) which leads to the change of the convective flux density, nv. In fig. 2 the edge convective and total flux densities are also displayed for Ne seeded and non-seeded discharges. Comparing Ne seeding with non seeding, one sees that the increase of the convective flux is dominant with respect to that of the source term, except in the very last 1-2 cm (minor radius a = 46 cm) where the density gradient becomes negative according to dn/dr = (1/D) x(-Γ+ nv).

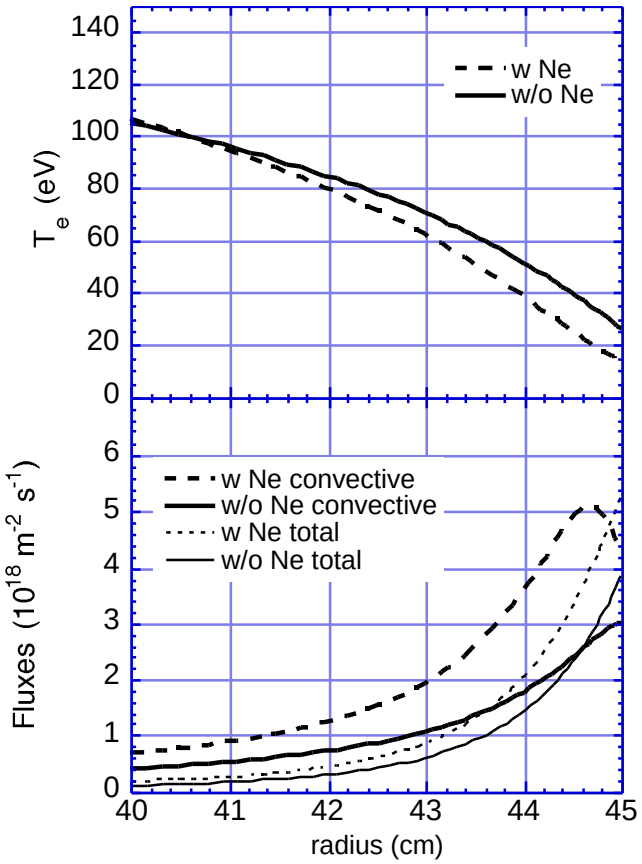

Fig.2 Edge electron temperature without and with Ne at n_{eo}= 8x10^{13}cm^{-3} (top) and edge total and convective flux densities without and with Ne at n_{eo}= 8x10^{13}cm^{-3} (bottom).

4. Results (Confinement)

In experiments and in RITM simulations, at a given plasma current the energy confinement increases with increasing electron density. In the frame of the transport model we have adopted, this trend appears to be dependent on the collisional term, since the magnetic fluctuation level, which is linked to the Lunquist number, generally increases with increasing density. Typically, for standard non-seeded RFX discharges the confinement time of the electronic channel τ_{Ee} ranges from 0.3 —0.4 ms at low density up to 0.5 — 0.6 ms at high density, in reasonable agreement with experimental findings.

The slight increase of the thermal stored energy of Ne seeded discharges with respect to the non-seeded ones, reported in the previous section, does not derive from a positive effect of neon seeding on confinement, but from the enhanced level of the input power P_{tot}. In fact, in the RFX plasmas, purely ohmically heated, the increased resistivity level associated with Ne

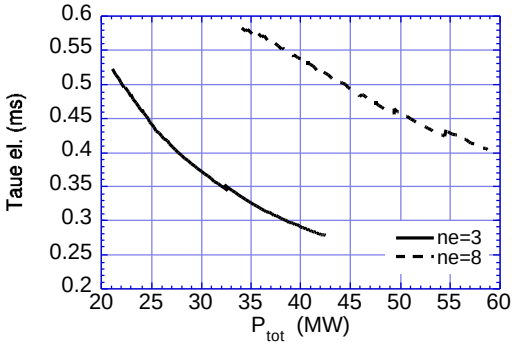

Fig. 3 Energy confinement time (electron channel) vs. input power at n_{eo}=3 and 8x10^{13}cm^{-3}.

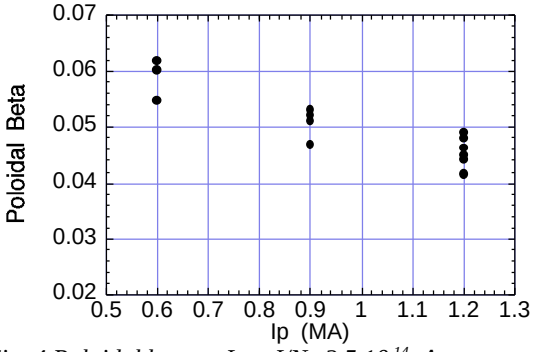

Fig. 4 Poloidal beta vs I_p at I/N=2.5 10^{-14} Am.

seeding (Zeff) leads to the rise of P_{tot} and to a reduced confinement. In fig. 3, τ_{Ee} is shown as a function of P_{tot} (where P_{tot} is increased by increasing the neon puffing rate) for discharges at n_{e0} = 3 x 10^{13} cm^{-3} and 8 x 10^{13} cm^{-3}. The range of P_{tot} and of τ_{Ee} in RITM simulations is comparable with the experimental one, both at low and at high density [9]. Since for any given incremental level of edge radiation, the corresponding incremental P_{tot} (and Zeff) scales approximately as $1/n_e^2$ [10], a minor increase of P_{tot} at high density leads to a significant increase in P_{rad} and of the power radiated ratio ($\gamma = P_{rad}/P_{tot}$). This ultimately allows the feasibility of a radiative mantel in high density plasmas without significant increase in the confinement losses. Since τ_{Ee} scales as $(Ptot)^{-\alpha}$ with α in the range 0.7 - 0.9, the total stored energy, as well as the poloidal beta changes slightly (up to 10 — 15%) when the full range of P_{tot} is scanned, at low and at high density.

When the plasma current is increased (so far Ip = 850 kA) and the electron density is raised so that Ip/N remains constant (N is the line density), the poloidal beta decreases slightly (see fig.4 where different points at a given I_p refer to different P_{tot}). This result, which is consistent with the experimentally determined scaling $\beta_p \propto n_e^{0.7}/I_p$ [9], contribute to the validation of the transport model adopted in RITM against observations of global parameters.

References

1. M.Z. Tokar, Plasma Phys. Controlled Fusion **36**, 1819 (1994).
2. M.Z. Tokar et al., Plasma Phys. Controlled Fusion **39**, 569 (1997).
3. S.Ortolani, Proc. Int. School on Mirror-based and Field Reversed approaches to Magnetic Fusion, Varenna Italy, Sept.1983, Vol.II Eds. E.D.Post, E.Sindoni
4. L. Marrelli et al., Nucl. Fusion **38**, 649 (1998).
5. A.B. Recester and M.N. Rosenbluth, Phys. Rev. Lett. 40 (1978) 38
6. F. DÕAngelo and R. Paccagnella, Plasma Phys. Control. Fusion 41 (1999) 941
7. M.Z. Tokar, Phys. Plasmas (1999)
8. D. Gregoratto et al., Nucl. Fusion 38 (1998) 1199
9. L. Carraro et al. Submitted for publication in Nuclear Fusion
10. G. Telesca et al. Journal.Nucl. Mater. 241-243b(1997) 853